Contract No.:

This manuscript has been authored by Savannah River Nuclear Solutions (SRNS), LLC under Contract No. DE-AC09-08SR22470 with the U.S. Department of Energy (DOE) Office of Environmental Management (EM).

Crystal growth of CdZnTeSe (CZTS) gamma detectors: A promising alternative to CdZnTe

U. N. Roy, G. S. Camarda, Y. Cui, R. Gul, A. Hossain, G. Yang and R. B. James*

Brookhaven National Laboratory, Upton, NY 11973, United States.

V. Lordi and J. Varley

Lawrence Livermore National Laboratory, Livermore, CA 94550, USA

J. Zazvorka, V. Dedic and J. Franc

Institute of Physics, Charles University, Ke Karlovu 5, Prague 121 16, Czech Republic

****Present address: Savannah River National Laboratory, Aiken, SC 29808, United States.***

70 YEARS OF DISCOVERY

A CENTURY OF SERVICE

U.S. DEPARTMENT OF ENERGY

BROOKHAVEN NATIONAL LABORATORY

SRNL-STI-2017-00526

Introduction

Cadmium zinc telluride (CZT) is the most advanced room-temperature semiconductor material for gamma-ray detection.

Disadvantages of CZT:

i) **Non-unity segregation of Zn in CdTe matrix causing a compositional gradient along ingots**
ii) **Sub-grain boundaries and their networks lowering the mu-tau product, and imposing spatial non-uniformity on the device's charge-transport properties**
iii) **Large number of Te inclusions/precipitates (about 2-8x10^5/cm^3) in CZT lowers the mu-tau product causing non-uniformity in the device's charge-transport properties/electric field inside the device**

- ***These issues cause low yield and high cost of CZT radiation detectors, limiting their applications.***
- ***Researchers have tried to solve the issues by improving the crystal growth process and post-growth annealing, but have not mitigated all disadvantages.***
- ***The main reason is poor thermo-physical properties of CdTe/CZT.***

Introduction

The proposed new quaternary semiconductor $Cd_{1-x}Zn_xTe_{1-y}Se_y$ (CZTS) is expected to resolve these long-standing problems associated with CZT material. Hence, high-performance detector-grade CZTS material can be potentially produced at lower cost.

Non-unity segregation coefficient of Zn (~1.35) in CdTe matrix

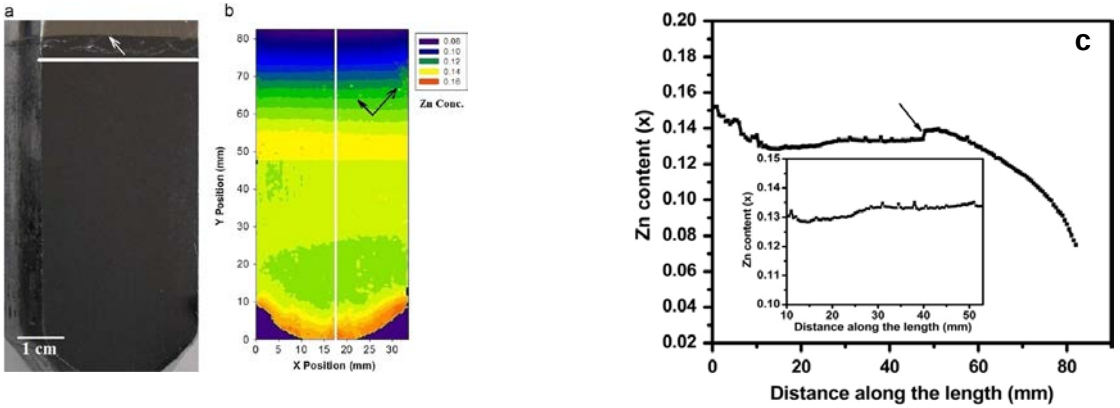

(a) THM-grown CZT ingot cut along the length, (b) Zn concentration mapping and (c) Zn concentration along the length of the ingot. *Roy et al. J. Crystal Growth 347 (2012) 53.*

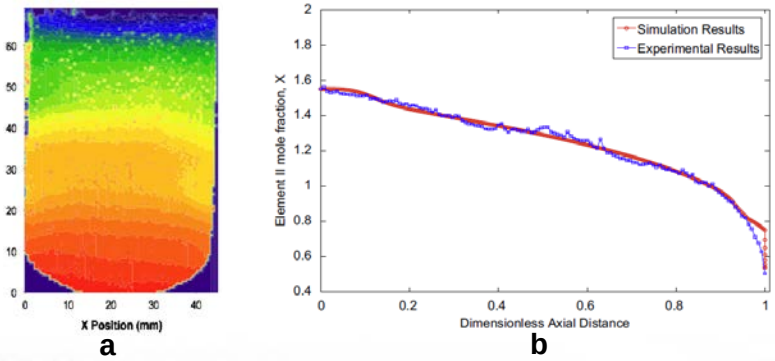

(a) Zn concentration mapping and b) Zn variation along the length of Bridgman-grown ingot. *J. Derby et al. J. Crystal Growth 325 (2011)10.*

Yield is highly compromised

Presence of large concentration of sub-grain boundaries and their network.

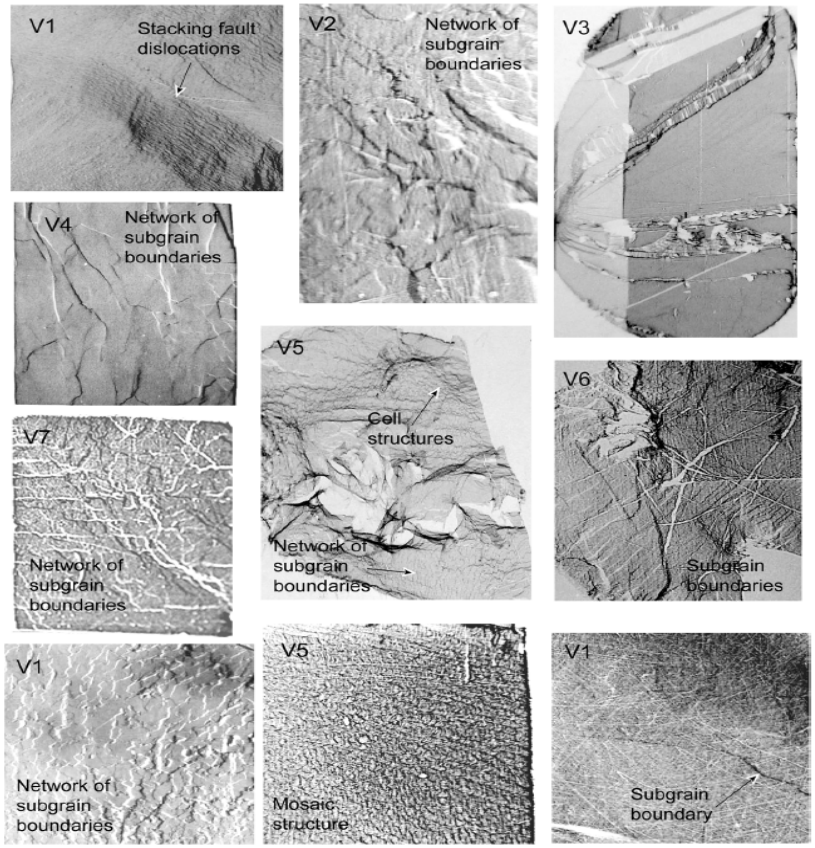

X-Ray diffraction topography images showing ~1 cm^2 areas of detector-grade CZT samples supplied by seven different vendors.

A. E. Bolotnikov et al. J. Cryst. Growth 379 (2013) 46.

Effect of sub-grain boundary and their network on CZT device response

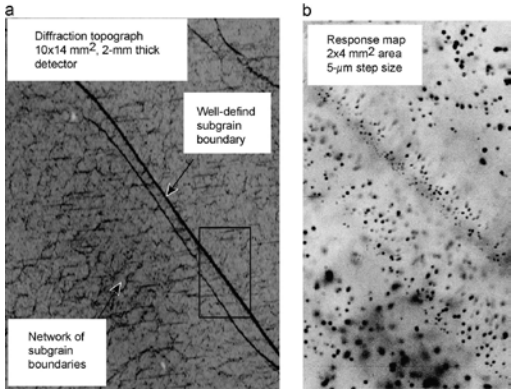

X-ray topography and the high-resolution X-ray response map

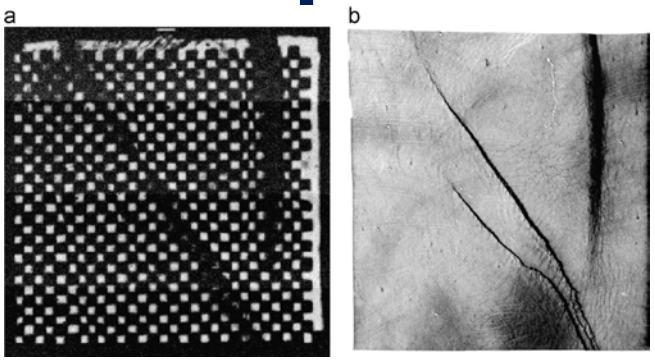

X-ray topography and the high-resolution X-ray response map of pixelated device (sample dimensions: 20x20x2 mm^3.

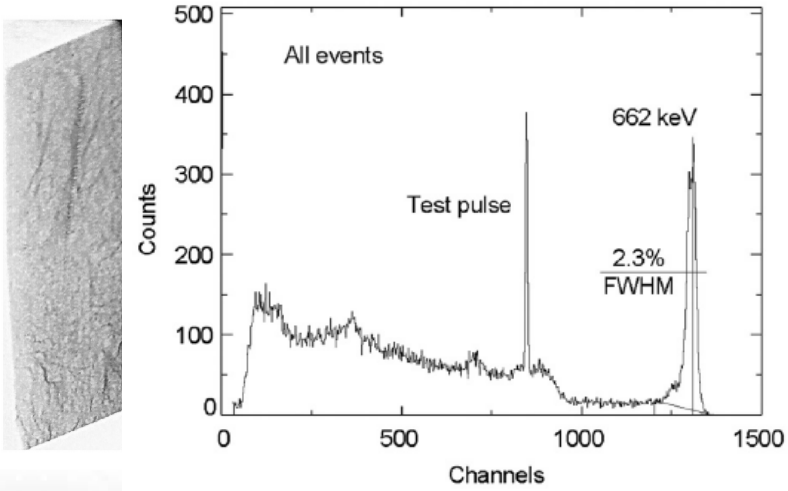

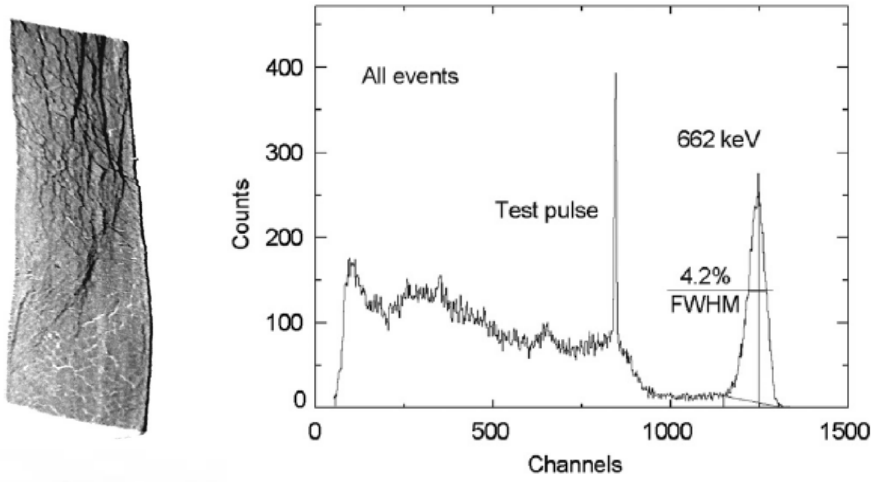

X-ray topography and the pulse height spectrum of CZT Frisch-grid detector. Sample dimensions: 6x6x15 mm^3.

A. E. Bolotnikov et al. J. Cryst. Growth 379 (2013) 46.

Effect of Te-inclusions/precipitates on CZT device response

FWHM (%) at 662 keV, of the cumulative effect of Te inclusions to energy resolution (after bi-parametric correction) versus their concentration calculated for 1-, 3-, 5-, 10-, and 20- μm inclusions. The detector's length is 15 mm.

A. E. Bolotnikov et al., IEEE Trans. on Nucl. Science 54, 821 (2007).

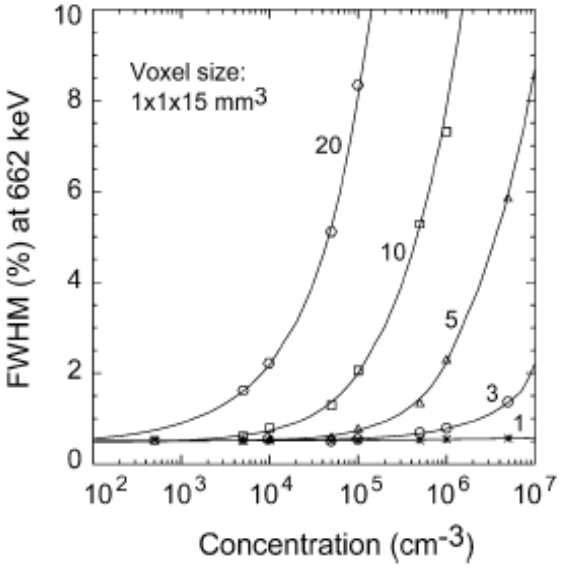

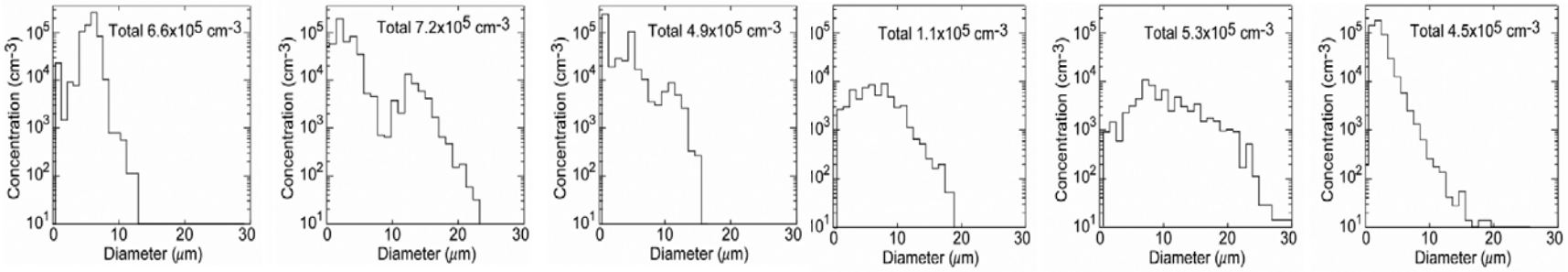

Size distribution and concentration of secondary phases for standard CZT from different vendors.

A. E. Bolotnikov et al., IEEE Trans. on Nucl. Science 57 (2010) 910.

Effects of thermal annealing on Te-inclusions in CZT

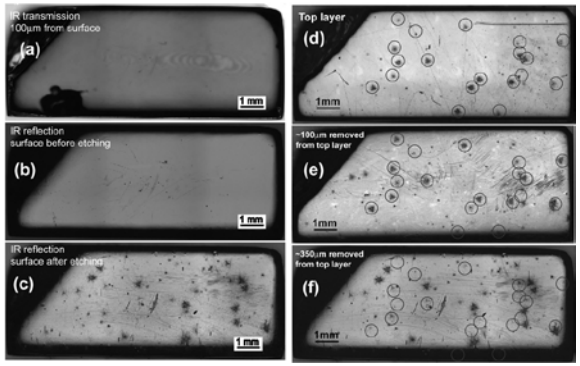

Star shaped defects after Cd annealing

A. Hossain et al., JCG 312 (2010) 1795.

WBXDT image

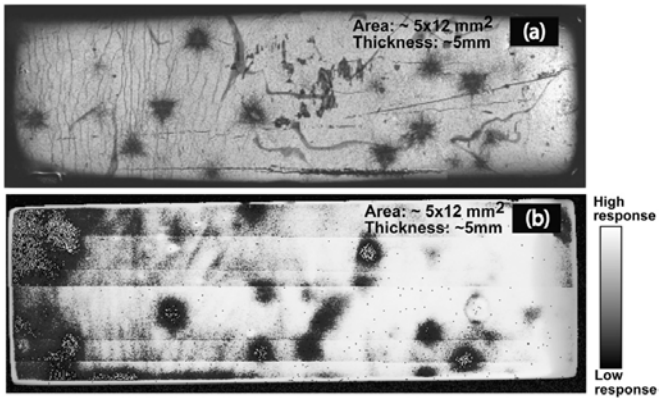

a) Etched surface of CZT crystal and b) X-ray response map. Punching defects after Cd annealing.

A. Hossain et al., JCG 312 (2010) 1795.

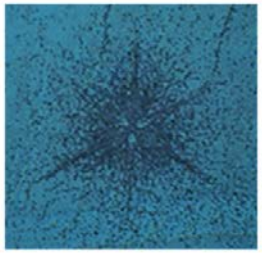

Optical image

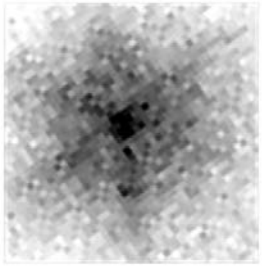

X-ray response map

Details of a 'star-like' defect revealed by optical microscopy imaging of the CZT crystal surface after chemical etching (left) and a map of the electron charge- collection efficiency after synchrotron X-ray response mapping (right).

G. E. Yang et al., JCG 379 (2013) 16.

Path to grow CZTS

- The safe path to choose the right compound to match CZT band gap (~1.57 eV for 10 at% Zn), keeping Se composition to be ~7 at%.

  The simple empirical formula for $Cd_{1-x}Zn_xTe_{1-y}Se_y$ quaternary compound is,

  $$Eg_{(x,y)} = 1.511-0.54y+ 0.6x \ (x, y \leq 0.10)$$

  and the corresponding compound is $Cd_{0.84}Zn_{.16}Te_{0.93}Se_{0.07}$.

- We decided to keep the Zn concentration to be ~ 10 at% (the challenging path), and vary the concentration of Se from 2-7 at%, in order to lower the concentration of Te inclusions/precipitates. (Disadvantage: lower band gap than CZT)

Phase diagram of CdTe and CZT

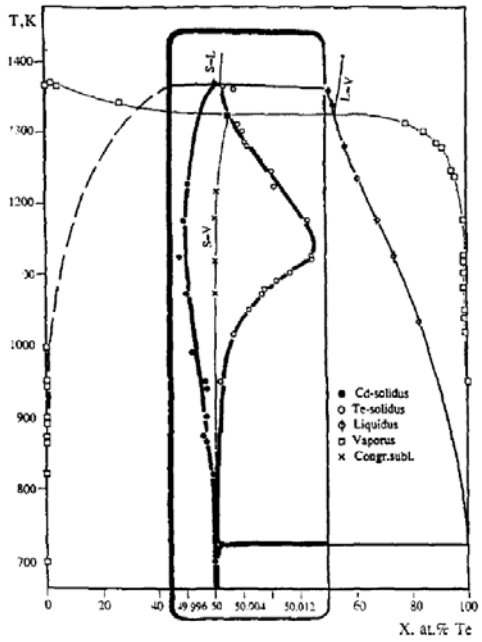

T-X projection of CdTe solidus

Taken from Greenberg, J. Cryst. Growth 161 (1996) 1.

Material	Temperature (°C)	x_s at% of Te
CdTe	~ 900	~ 50.014
$Cd_{0.9}Zn_{0.1}Te$	~ 900	~ 50.052
$Cd_{0.85}Zn_{0.15}Te$	~ 900	~ 50.1

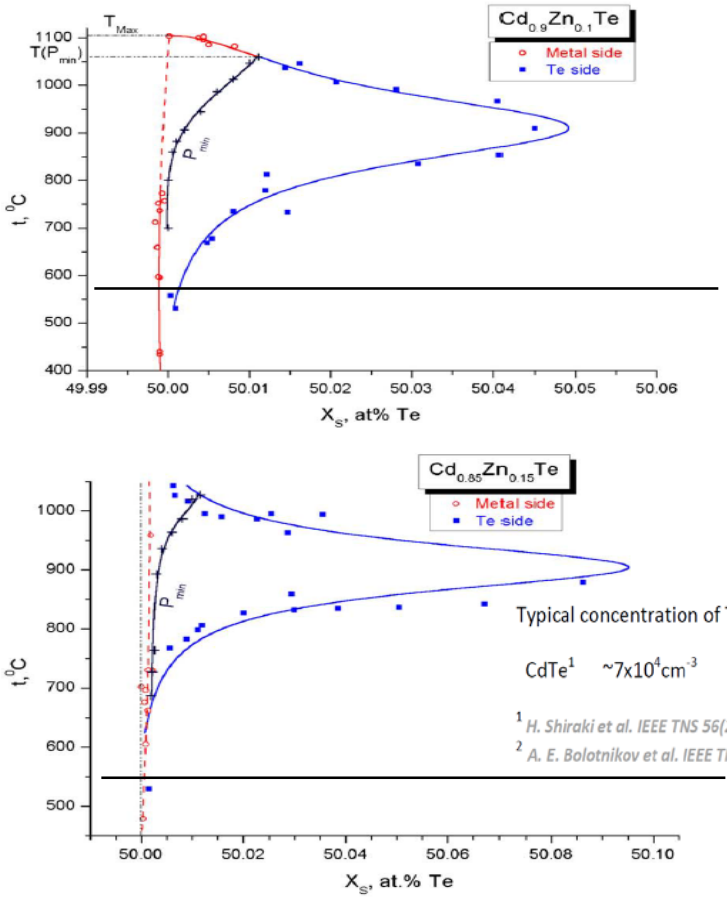

Typical concentration of Te inclusion/precipitation in CdTe and CZT

CdTe[1] ~$7x10^4 cm^{-3}$ CdZnTe (10 at% Zn)[2] 2-$8x10^5 cm^{-3}$

[1] *H. Shiraki et al. IEEE TNS 56(2009)1717*

[2] *A. E. Bolotnikov et al. IEEE TNS 57(2010)910.*

T-X projection of $Cd_{0.9}Zn_{0.1}Te$ and $Cd_{0.85}Zn_{0.15}Te$ solidus

Taken from Greenberg and Guskov, J. Cryst. Growth 289 (2006) 552.

1. Higher Zn concentration: higher concentration of Te inclusions/precipitates.

2. Higher Zn concentration: higher alloy broadening.

Growth and characterization

- CZTS ingots were grown by traveling heater method (THM) as well as vertical Bridgman Method (BM).
  - 6N purity CdZnTe and CdSe were used for synthesis of the CZTS compound.
  - 6N purity Te was used as solvent for THM growth.
- Although BM technique has higher growth rate and is being used for crystal growth, our main thrust is THM growth of CZTS for its following advantages:
  - Low-temperature growth
  - Less chance of incorporation of impurities from the crucible during growth
  - Less/no chance of ampoule explosion
  - Enhanced purity of the ingot
  - Fewer defects due to the lower growth temperature
- Crystals were cut and polished for various characterizations and detector fabrication and testing.

Optimizing THM-growth parameters

THM growth is highly sensitive to growth parameters.

i. **Width of Te-rich solution zone**
ii. **Growth temperature**
iii. **Temperature gradient near the growth interface**

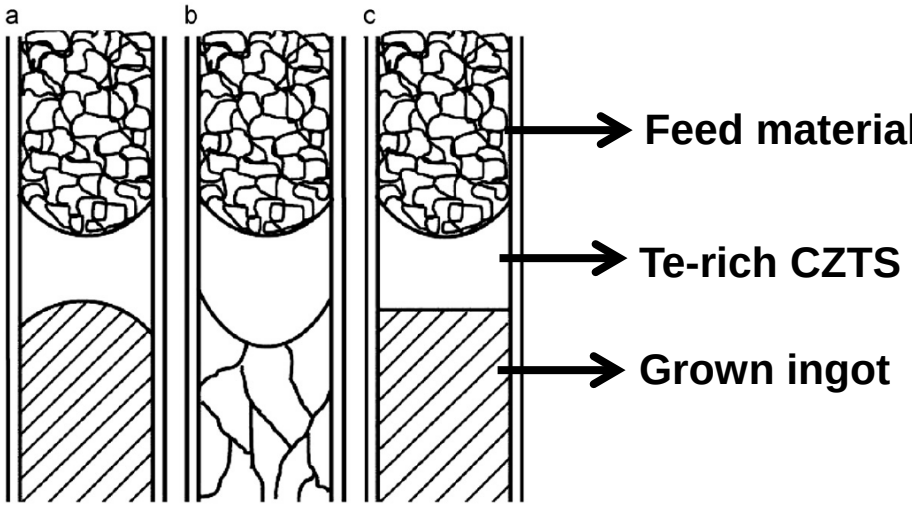

Schematic of growth interface shape A) convex, B) concave and C) flat.

Convex and flat growth interfaces are favorable for growth of large grain and single crystalline ingots.

Flat interfaces are desired for seeded growth.

CZTS ingots

- We are focusing on THM-growth of 2-in diameter CZTS ingots with different elemental compositions:

$Cd_{0.9}Zn_{0.1}Te_{0.93}Se_{0.07}$ ingots:

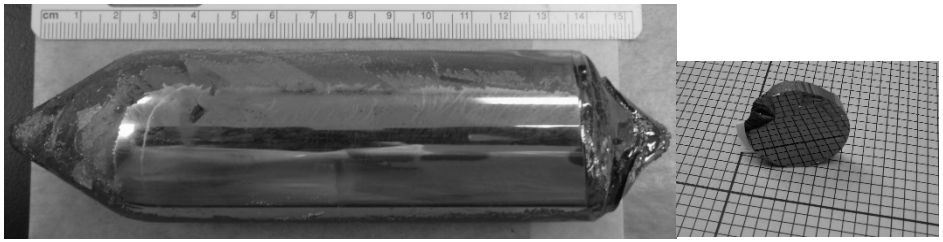

40-mm diameter ingot grown by BM (undoped).

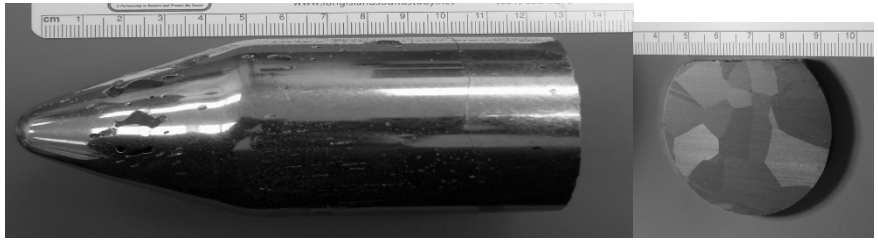

In-doped 52-mm diameter ingot grown by THM (fast cooled ingot).

$Cd_{0.9}Zn_{0.1}Te_{0.96}Se_{0.04}$ ingots:

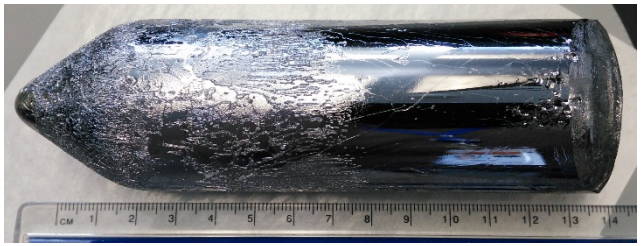

40-mm diameter ingot grown by BM (undoped).

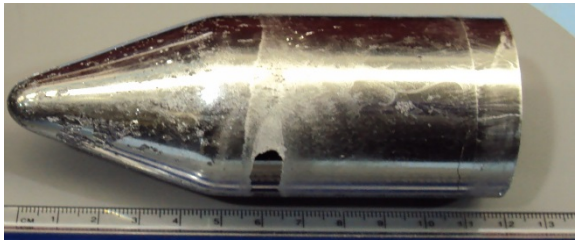

In-doped 52-mm diameter ingot grown by THM.

$Cd_{0.9}Zn_{0.1}Te_{0.98}Se_{0.02}$ ingots:

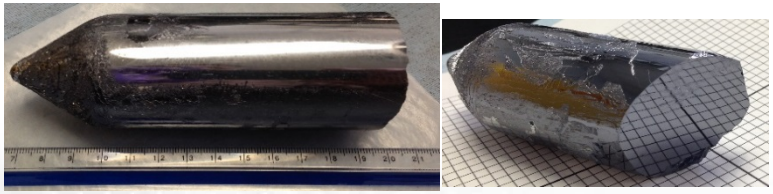

40-mm diameter ingot grown by BM (undoped).

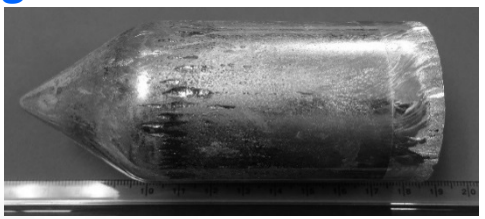

In-doped 52-mm diameter ingot grown by THM.

Growth interface (THM)

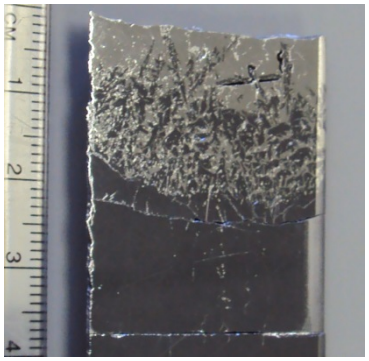

Concave interface of 52-mm diameter $Cd_{0.9}Zn_{0.1}Te_{0.93}Se_{0.07}$ ingot grown by THM.
The very first CZTS ingot.

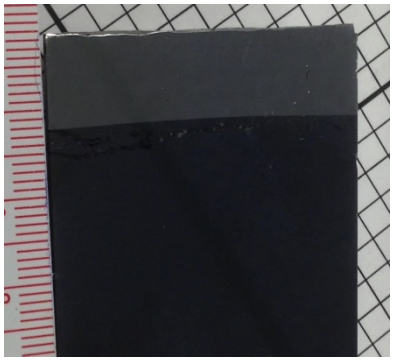

Slightly convex nearly flat interface of 52-mm diameter $Cd_{0.9}Zn_{0.1}Te_{0.98}Se_{0.02}$ ingot grown by THM.

Slightly convex nearly flat interface of 52-mm diameter $Cd_{0.9}Zn_{0.1}Te_{0.96}Se_{0.04}$ ingot grown by THM.

Since our goal is seeded growth, we are focusing on achieving slightly convex and nearly flat growth interface.

Compositional distributions in CZTS

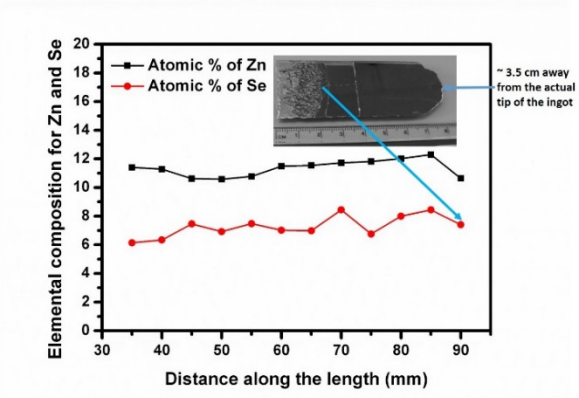

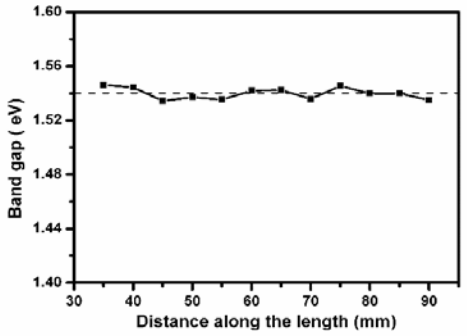

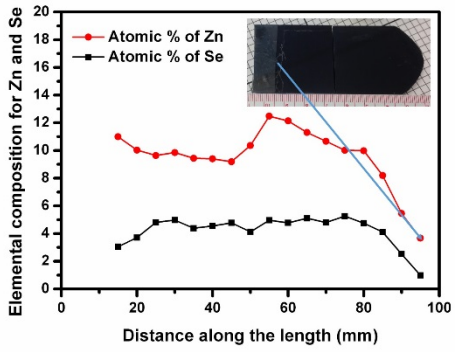

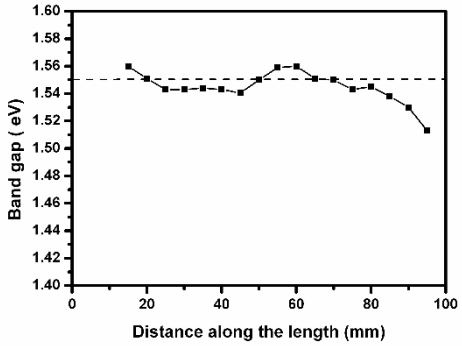

Zn and Se composition and the calculated band gap along the length of the THM-grown $Cd_{0.9}Zn_{0.1}Te_{0.93}Se_{0.07}$ (top), and $Cd_{0.9}Zn_{0.1}Te_{0.96}Se_{0.04}$ (bottom) ingots.

Composition of Zn and Se is fairly uniform throughout the ingot for $Cd_{0.9}Zn_{0.1}Te_{0.93}Se_{0.07}$. Especially the calculated band gap.

For 4% Se composition, the band gap of the ingots is fairly uniform within the experimental accuracy. It only decreases in a narrow region (< 1 cm) near the interface.

(~90% of the ingot shows uniform band gap for 4% Se composition).

On the contrary, for THM grown CZT, only about one third of the ingot shows uniform composition.

Bridgman grown CZTS

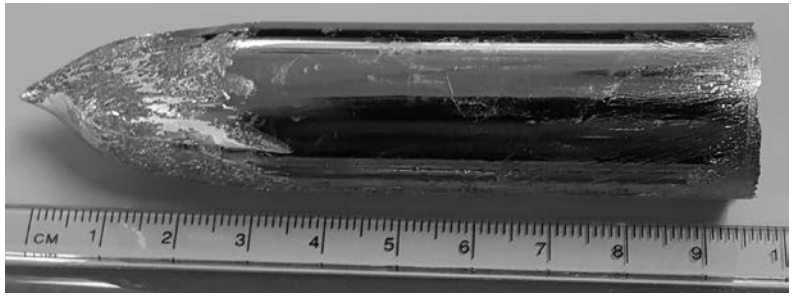

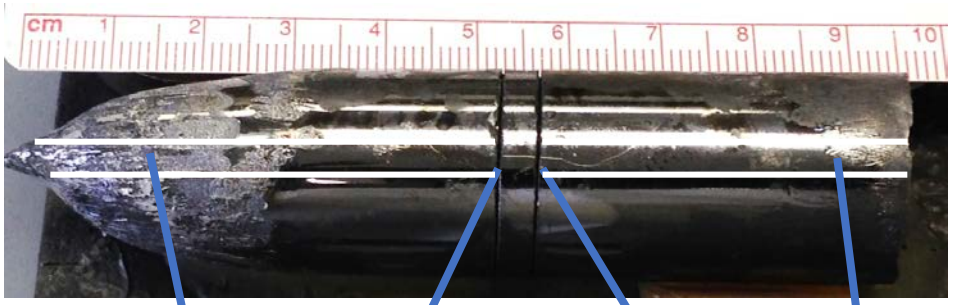

Typical 22-mm diameter $Cd_{0.9}Zn_{0.1}Te_{0.96}Se_{0.04}$ ingot grown by the Bridgman technique.

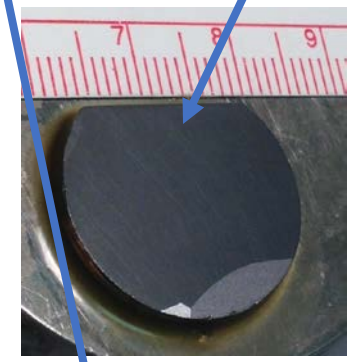

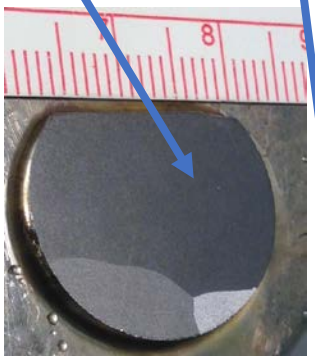

Two surfaces of a wafer from center of the ingot

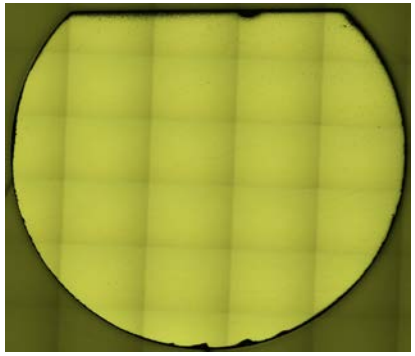

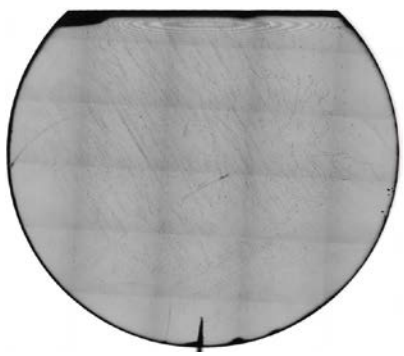

Cross-sectional wafer in reflection mode (left) and IR transmission image (right)

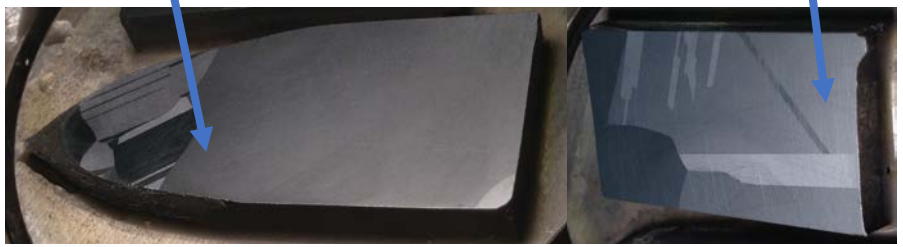

Photograph of the longitudinal wafers

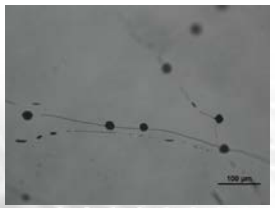

Typical IR transmission microscopic image showing Te inclusions/precipitates

Room-temperature PL map of $Cd_{0.9}Zn_{0.1}Te_{0.93}Se_{0.07}$ 2-inch wafer

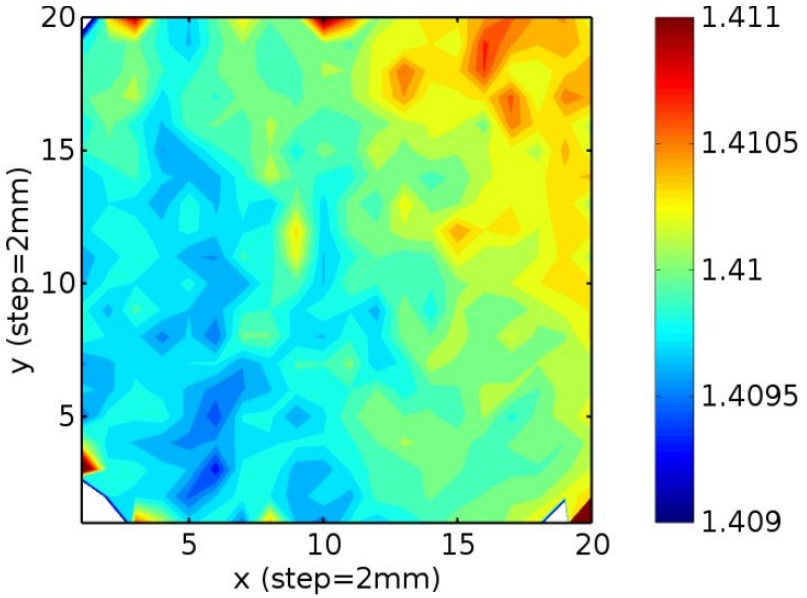

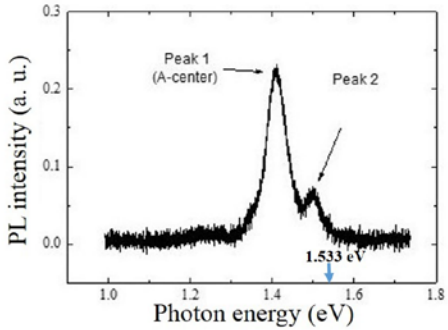

Room temperature photoluminescence (PL) map of $Cd_{0.9}Zn_{0.1}Te_{0.93}Se_{0.07}$ two inch wafer grown by THM. The map area is 4 x 4 cm².

The room-temperature PL spectrum shows A-center peak (peak 1). Peak 2 is unknown and possibly due to donor-acceptor pair (DAP) transition. The band gap of this sample is ~1.533 eV. However, the uniformity of Peak 1 position in the plot should track the uniformity of the band gap.

The energy position of peak 1 was registered across a 4x4-cm² area as shown in the figure. Variation of the peak energy over the entire scanned area, *ΔE is ~ 2 meV*, thus the composition is highly uniform over the 4x4-cm² area.

In general, the A-center is ~0.12-0.15 eV away from the valence band maximum. Peak 1 is at ~1.41 eV, thus the band gap of the sample is ~1.54 eV.

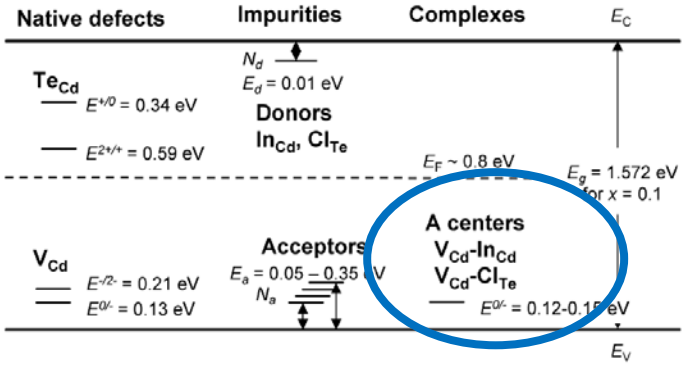

Position of the ionization energy levels of native defects, impurities, and defect complexes in semi-insulating $Cd_{1-x}Zn_xTe$

C. Szeles, IEEE TNS 51(2004) 1242

Composition is highly uniform

X-ray Topographic Analyses of $Cd_{0.9}Zn_{0.1}Te_{0.93}Se_{0.07}$

All the topographic experiments were carried out on mirror finish polished surfaces, followed by etching in freshly made 2% Bromine-methanol solution, for 2 minutes.

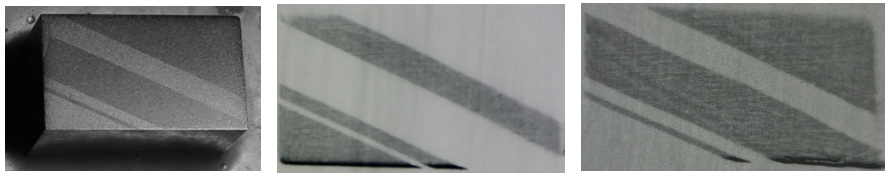

Samples are almost stress free

Optical photograph and X-ray topographic pictures of Bridgman grown $Cd_{0.9}Zn_{0.1}Te_{0.93}Se_{0.07}$ sample of dimensions 5x6x11 mm^3

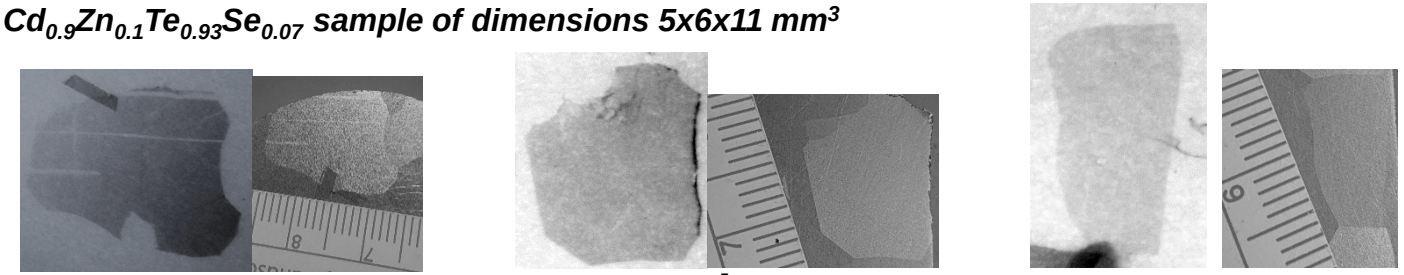

a **b** **c**

a)- c): X-ray topographic pictures of THM-grown $Cd_{0.9}Zn_{0.1}Te_{0.93}Se_{0.07}$ (fast cooled) sample and the corresponding optical photography of the grains.

Sub-grain boundaries and their networks were not observed for the composition of 7% Se.

Appearance of the twins without any deformation in topography indicates no/less residual thermal stress.

X-ray Topographic Analyses of THM Grown $Cd_{0.9}Zn_{0.1}Te_{0.96}Se_{0.04}$

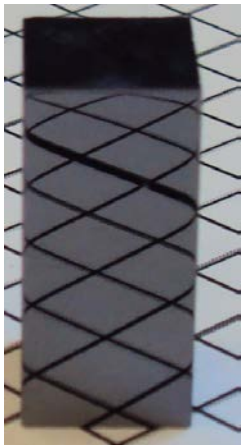

Photograph of the sample, dimensions of the area exposed: 21x9 mm²

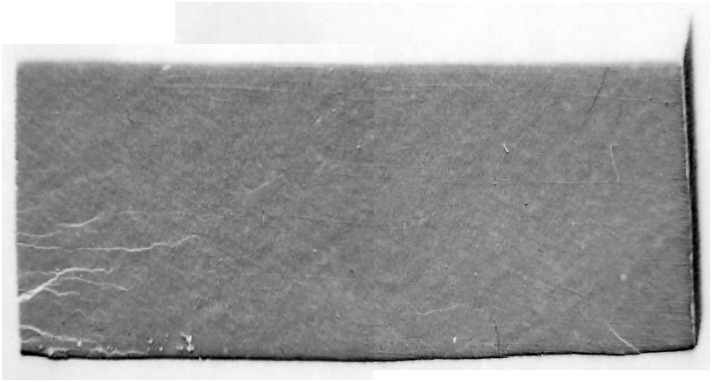

X-ray topographic picture of the THM-grown $Cd_{0.9}Zn_{0.1}Te_{0.96}Se_{0.04}$ sample

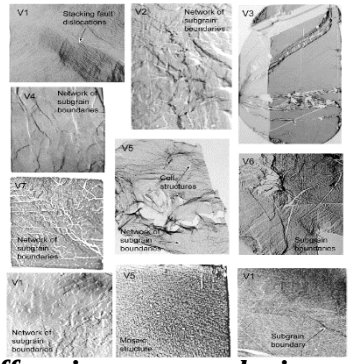

X-Ray diffraction topography images showing ~1 cm² areas of detector-grade CZT samples supplied by seven different vendors.

A. E. Bolotnikov et al. J. Cryst. Growth 379 (2013) 46.

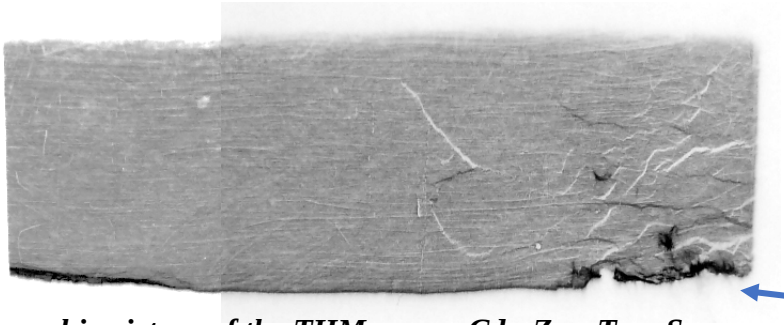

X-ray topographic picture of the THM-grown $Cd_{0.9}Zn_{0.1}Te_{0.96}Se_{0.04}$ sample

Damaged area

Photograph of the sample, dimensions of the area exposed: 21x7.85x7.95 mm³

Few sub-grain boundaries are evident from the shown X-ray topographic pictures, while no sub-grain boundary network was observed.

U.S. DEPARTMENT OF ENERGY | BROOKHAVEN NATIONAL LABORATORY

70 YEARS OF DISCOVERY
A CENTURY OF SERVICE

Presence of Secondary phases in THM Grown *CZTS (IR Transmission Microscopy)*

High magnification IR transmission microscopic image $Cd_{0.9}Zn_{0.1}Te_{0.96}Se_{0.04}$ ingot (1st ingot)

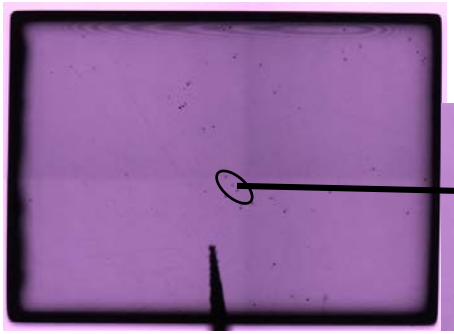

IR transmission picture of the THM grown $Cd_{0.9}Zn_{0.1}Te_{0.96}Se_{0.04}$ sample, sample dimensions: 6.9x5x1.7 mm^3

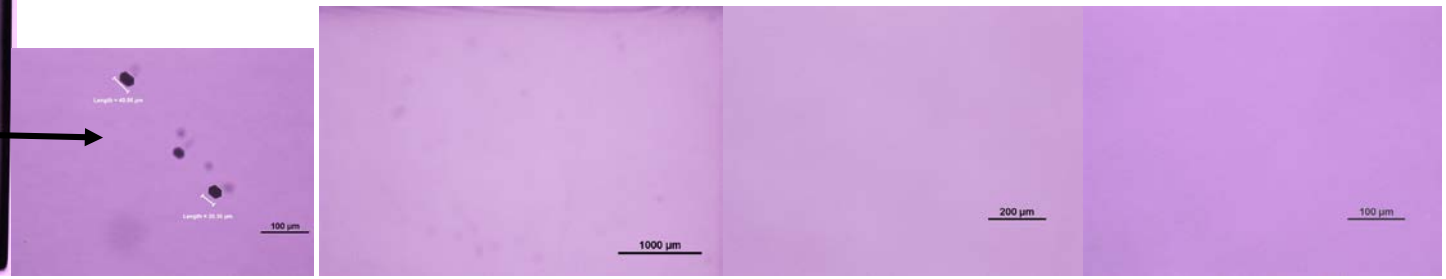

High magnification IR transmission microscopic images

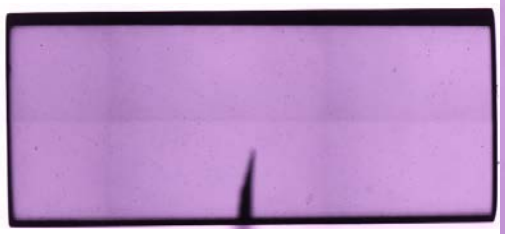

IR transmission picture of the THM grown $Cd_{0.9}Zn_{0.1}Te_{0.96}Se_{0.04}$ sample, sample dimensions: 4.6x4.5x10.7 mm^3

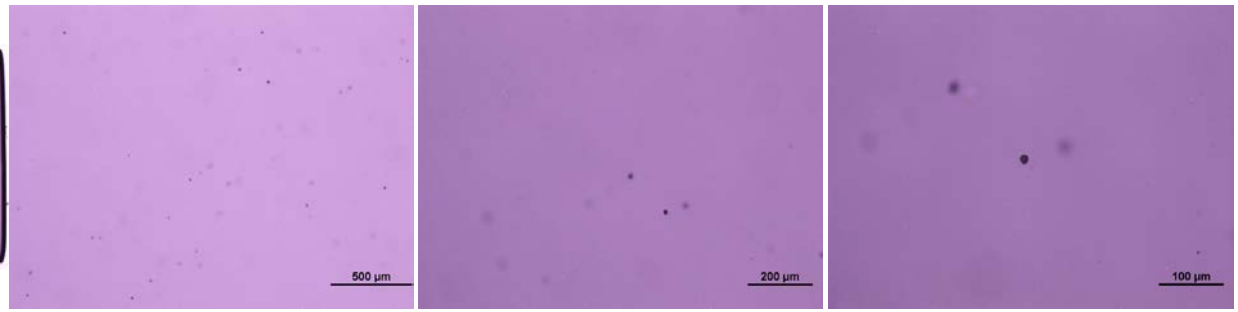

High magnification IR transmission microscopic images

Presence of Secondary Phases in THM Grown *CZTS (IR Transmission Microscopy)*

Quantitative evaluation of size distribution of Te inclusions/precipitates for $Cd_{0.9}Zn_{0.1}Te_{0.98}Se_{0.02}$ and $Cd_{0.9}Zn_{0.1}Te_{0.96}Se_{0.04}$ ingots will be performed soon.

High magnification IR transmission microscopic image $Cd_{0.9}Zn_{0.1}Te_{0.96}Se_{0.04}$ ingot (2nd ingot)

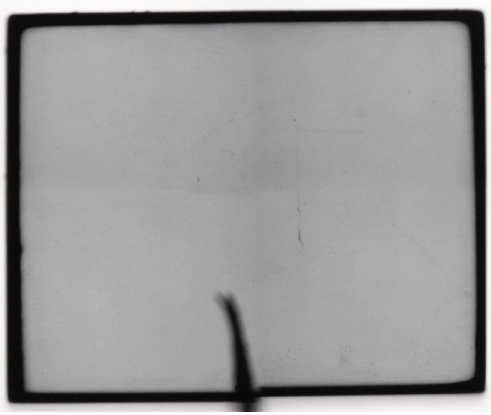

IR transmission picture of the THM grown $Cd_{0.9}Zn_{0.1}Te_{0.96}Se_{0.04}$ sample, sample dimensions: 6.5x5.3x2.68 mm^3

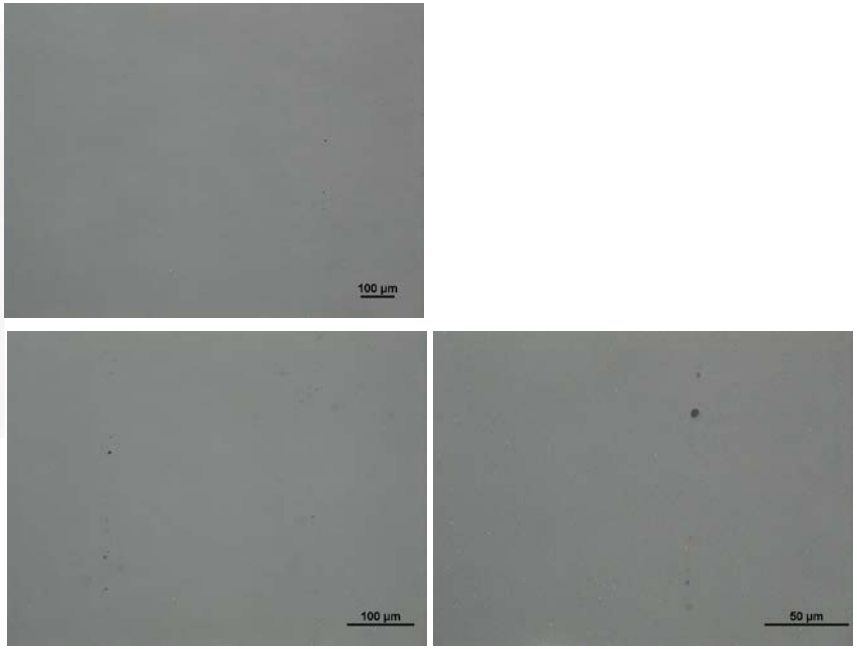

High magnification IR transmission microscopic images

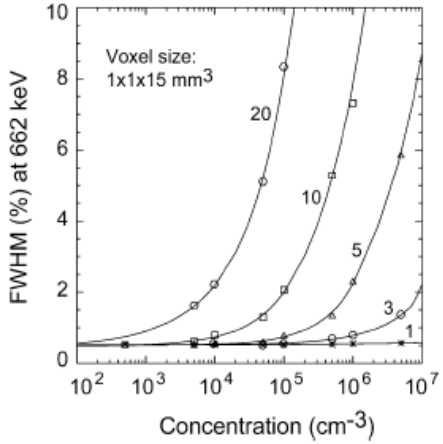

Not many inclusions > 20 µm are present in the CZTS samples.

Apparently Se seems to be effective in reducing the concentration of Te inclusions/precipitations.

Roles of Se in CZT matrix

Se helps

- **Modify Zn segregation coefficient**
  - *Uniform material*
  - *High yield*
- **Effective solution hardening to arrest sub-grain boundaries and their networks.**
  - *Less defects*
  - *High yield*
- **Reduce Te-inclusion/precipitate concentration with increased Se content.**
  - *Less defects*
  - *High yield*
- **Reduce charge trapping centers.**
  - *Better detector performance*

Charge transport properties of THM-grown $Cd_{0.9}Zn_{0.1}Te_{0.96}Se_{0.04}$

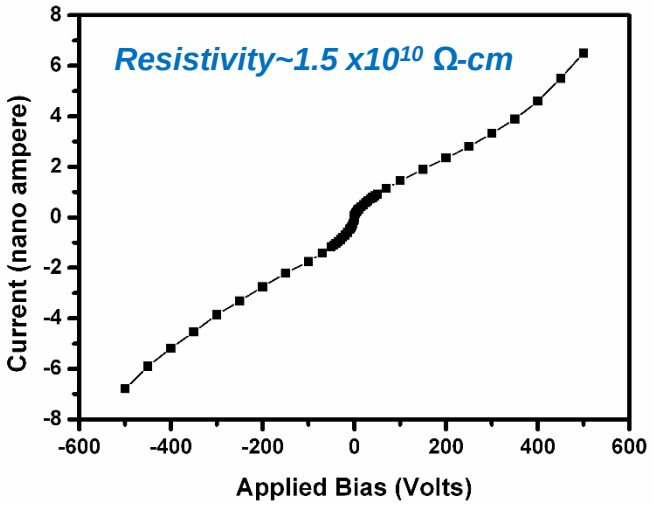

I-V characteristics at room temperature. Inset: I-V for 0-1V. Sample dimensions: 7x4.65x2.7mm³

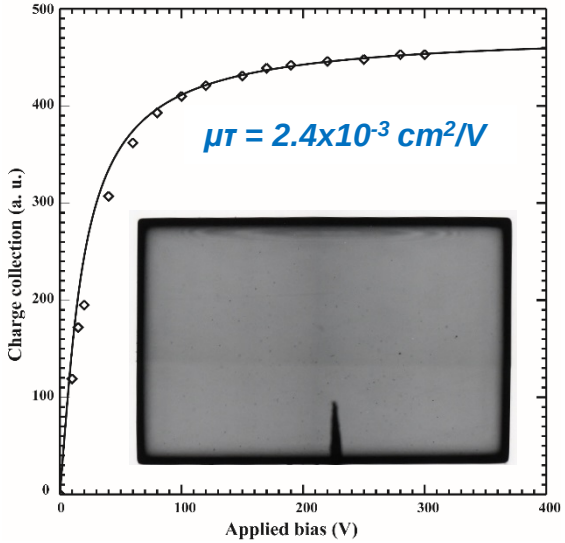

Charge collection versus applied bias
Inset: IR transmission picture of the sample

Across ~2.5 cm along the length of the ingot, the resistivity was found to be the same and the value of μτ as well.

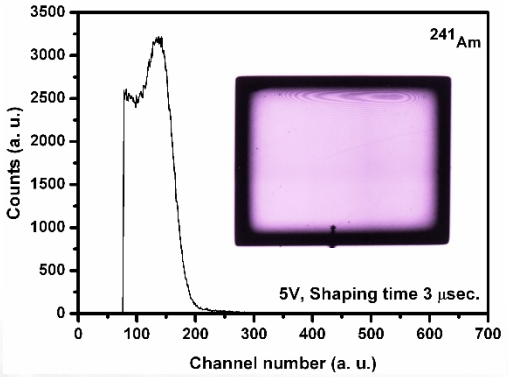

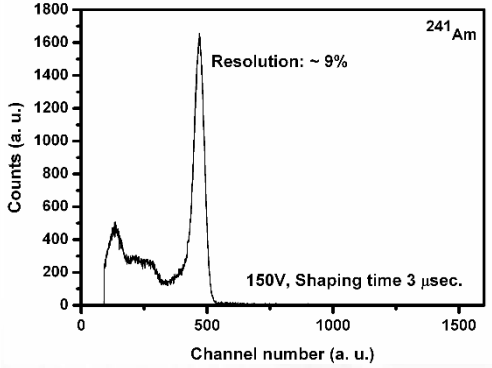

Pulse height spectra for ^{241}Am gamma source at room temperature. Sample dimensions: 5.15x4.25x1.48 mm³

For two ingots of THM-grown $Cd_{0.9}Zn_{0.1}Te_{0.96}Se_{0.04}$ the resistivity and $\mu\tau_e$ products are very similar.

Charge transport properties of THM-grown $Cd_{0.9}Zn_{0.1}Te_{0.98}Se_{0.02}$

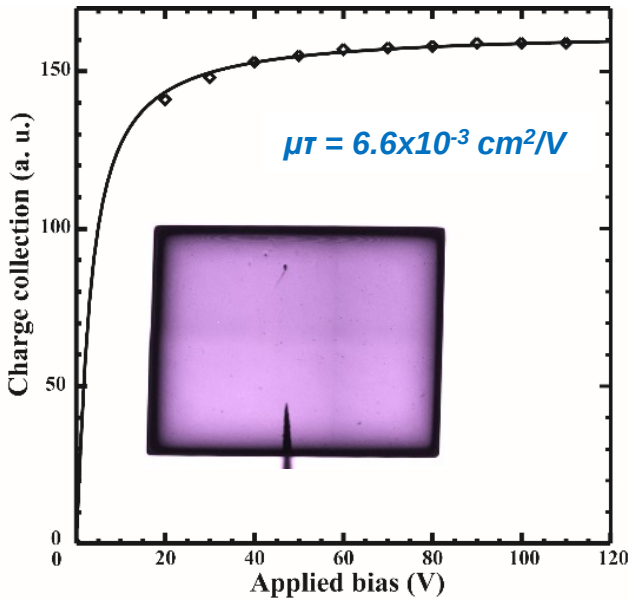

- *^{241}Am source*
- *Planar detector: 6.65x5.75x1.86 mm^3*

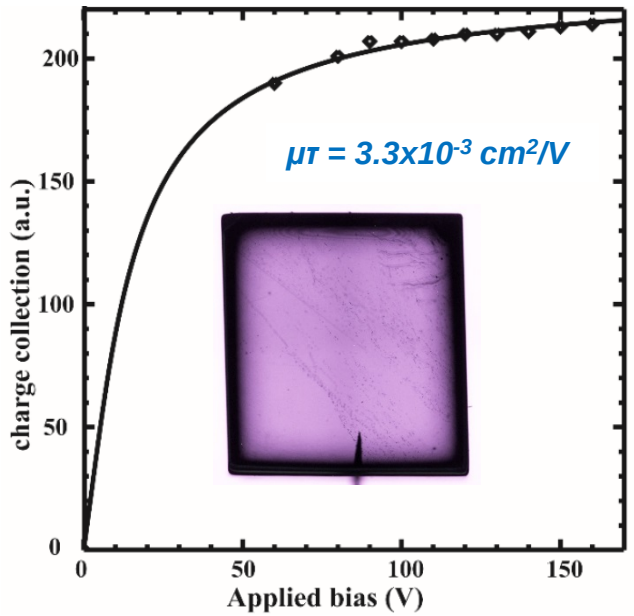

- *^{241}Am source*
- *Planar detector: 5.65x5.18x2.8 mm^3*
- *Sample with more Te-inclusions/precipitations*

In general the μτ product varies between 4.5-5 x10^{-3} cm^2/V.

Resistivity obtained: 1-3 x10^{10} Ω-cm

Detector response of quasi-hemispherical geometry

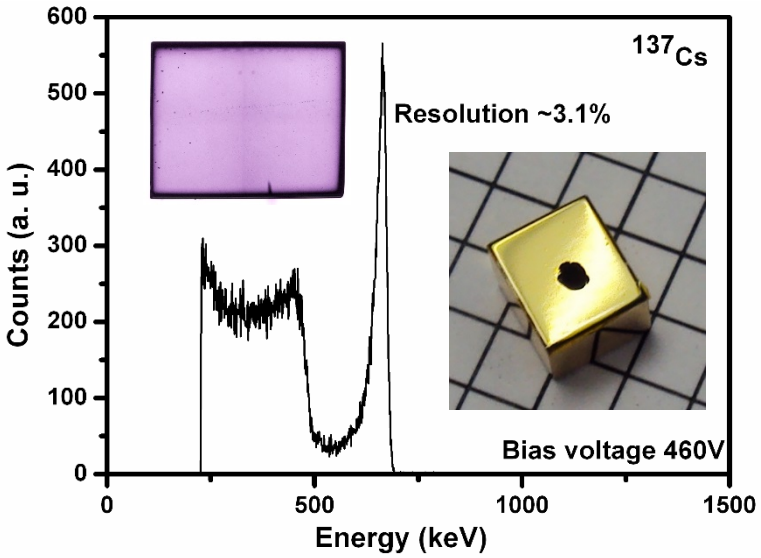

^{137}Cs response of a $Cd_{0.9}Zn_{0.1}Te_{0.98}Se_{0.02}$ quasi-hemispherical detector at room temperature

Resolution: ~3.1% at 662 keV

Bias: 460 V

Inset: Photograph of the detector and IR transmission image

Sample dimensions: 7.34x6.35x4.4 mm^3

The first Frisch-grid detector - THM-grown $Cd_{0.9}Zn_{0.1}Te_{0.98}Se_{0.02}$

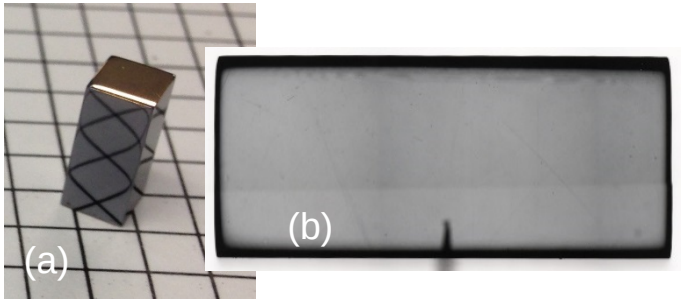

(a) Photograph of the detector 4.4x4.4x10 mm³
(b) IR transmission image

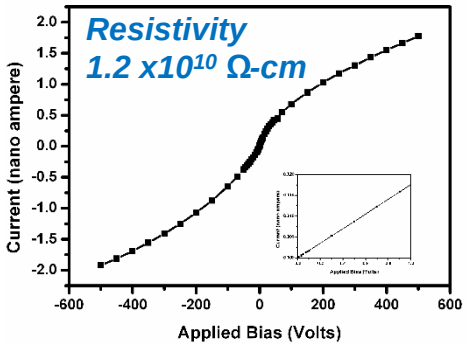

I-V characteristics at room temperature. Inset: I-V for 0-1V.

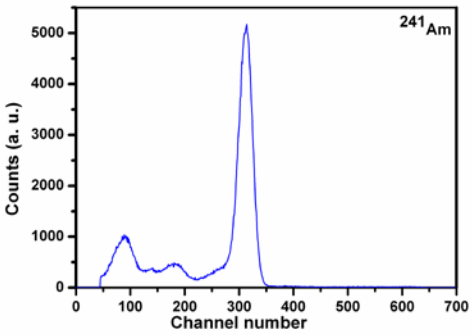

Bias voltage: -1800 V

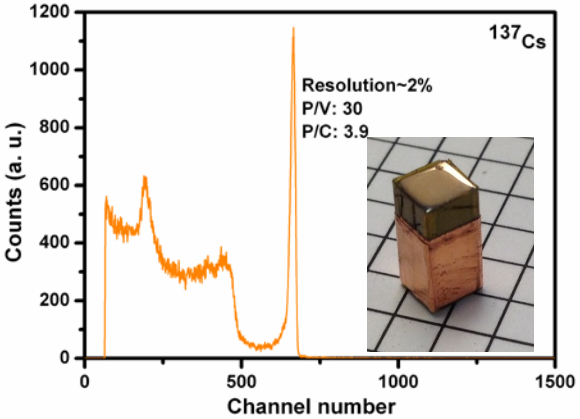

Bias voltage: -2300 V, (Frisch grid ~7mm long)

(The spectrum is as-measured)

- *All the charge transport characteristics and the detector responses are performed on **as-grown** THM CZTS ingots.*
- *No post-growth annealing.*

Advantages of CZTS

- **Se was found to be very effective in:**

i) **arresting the sub-grain boundaries**
ii) **better compositional homogeneity and**
iii) **lowering the concentration of secondary phase**

- **High μτ value was obtained with required resistivity.**
- **CZTS looks promising and has potential to supersede presently available CZT in terms of quality and yield at lower cost of production.**

Thank you for your kind attention !